Dimeric plant RhoGAPs are regulated by its CRIB effector motif to stimulate a sequential GTP hydrolysis

ARTICLE *in* JOURNAL OF MOLECULAR BIOLOGY · JUNE 2011

Impact Factor: 4.33 · DOI: 10.1016/j.jmb.2011.06.033 · Source: PubMed

4 AUTHORS, INCLUDING:

Antje Schaefer
Sanquin Blood Supply Foundation
10 PUBLICATIONS **73** CITATIONS
SEE PROFILE

Antje Berken
Max Planck Institute for Brain Research
21 PUBLICATIONS **607** CITATIONS
SEE PROFILE

doi:10.1016/j.jmb.2011.06.033 J. Mol. Biol. (2011) 411, 808–822

Contents lists available at www.sciencedirect.com

Journal of Molecular Biology

journal homepage: http://ees.elsevier.com.jmb

Dimeric Plant RhoGAPs Are Regulated by Its CRIB Effector Motif to Stimulate a Sequential GTP Hydrolysis

Antje Schaefer, Mandy Miertzschke, Antje Berken and Alfred Wittinghofer*

Department of Structural Biology, Max Planck Institute of Molecular Physiology, Otto-Hahn Str. 11, 44227 Dortmund, Germany

Received 21 April 2011; received in revised form 16 June 2011; accepted 16 June 2011
Available online 23 June 2011

Edited by I. Wilson

Keywords:
CRIB effector;
G protein;
GTPase-activating protein;
Pi release;
RopGAP

RopGAPs are GTPase-activating proteins (GAPs) for plant Rho proteins (ROPs). The largest RopGAP family is characterized by the plant-specific combination of a classical RhoGAP domain and a Cdc42/Rac interactive binding (CRIB) motif, which, in animal and fungi, has never been found in GAPs but in effectors for Cdc42 and Rac1. Very little is known about the molecular mechanism of the RopGAP activity including the regulatory role of the CRIB motif. Previously, we have shown that they are dimeric and form a 2:2 complex with ROPs. Here, we analyze the kinetics of the GAP-mediated GTP hydrolysis of ROPs using wild-type and mutant RopGAP2 from *Arabidopsis thaliana*. For an efficient GAP activity, RopGAP2 requires both the catalytic Arg159 in its GAP domain indicating a similar catalytic machinery as in animal RhoGAPs and the CRIB motif, which mediates high affinity and specificity in binding. The dimeric RopGAP2 is unique in that it stimulates ROP·GTP hydrolysis in a sequential manner with a 10-fold difference between the hydrolysis rates of the two active sites. Using particular CRIB point and deletion mutants lead us to conclude that the sequential mechanism is likely due to steric hindrance induced by the Arg fingers and/or the CRIB motifs after binding of two ROP molecules.

Introduction

Guanine nucleotide binding proteins (G proteins) are involved in cellular processes such as protein biosynthesis, membrane trafficking and organization of the cytoskeleton. These molecular switches cycle between a GDP-bound inactive state and a GTP-bound active state in a strictly regulated manner.[1,2] In contrast to septins, signal recognition particle, MnmE, and dynamin, which are activated

*Corresponding author. E-mail address: alfred.wittinghofer@mpi-dortmund.mpg.de.

Present addresses: A. Schaefer, Department of Molecular Cell Biology, Sanquin Research and Landsteiner Laboratory, Academic Medical Center, University of Amsterdam, Plesmanlaan 125, 1066 CX Amsterdam, The Netherlands; A. Berken, Department of Neural Systems and Coding & Synaptic Plasticity, Max Planck Institute for Brain Research, Deutschordenstr. 46, 60528 Frankfurt am Main, Germany.

Abbreviations used: CRIB, Cdc42/Rac interactive binding; GAP, GTPase-activating protein; mant (m), *N*-methylanthraniloyl; MDCC-PBP, phosphate-binding protein labeled with *N*-[2-(1-maleimidyl)ethyl]-7-(diethylamino) coumarin-3-carboxamide; ROP, Rho of plants; RopGAP, GAP for ROP; G protein, guanine nucleotide binding protein; GEF, guanine nucleotide exchange factor; GBD, G protein binding domain; WASP, Wiskott–Aldrich syndrome protein; WT, wild-type; AlFx, aluminum fluoride; PDB, Protein Data Bank.

by a nucleotide-dependent dimerization, conventional G proteins such as Ras, Rho, and Rap are controlled by specific interacting factors.[3] Guanine nucleotide exchange factors (GEFs) catalyze the nucleotide release by reducing the nucleotide affinity.[1] Since the cellular concentration of GTP is much higher than that of GDP, GEFs activate G proteins by facilitating GTP binding. The inactivation of G proteins is stimulated through GTPase-activating proteins (GAPs), which accelerate the slow intrinsic GTP hydrolysis by several orders of magnitude, based on complementation and/or stabilization of the active site. Many GAPs such as RasGAP,[4] RhoGAP,[5] RabGAP,[6] the ArfGAP ASAP3,[7] and the ArlGAP RP2[8] introduce an Arg residue (Arg finger) *in trans* into the active site of the cognate G protein to neutralize the developing negative charge during GTP hydrolysis and thus to stabilize the transition state. Moreover, a common principle is the correct positioning of the attacking water by a Gln residue. While this residue is supplied *in cis* by the switch II region of Ras, Rho, Arf, and Arl, it is donated *in trans* by the TBC domain of RabGAP. Following an alternative mechanism, RapGAP uses a conserved Asn *in trans* to orient the nucleophilic water.[9,10]

G proteins in the active GTP form interact specifically with effectors to ensure downstream signaling. Effectors have a G protein binding domain (GBD) in common although they differ in sequence, structure, and function. One important group of Rho effectors is characterized by the presence of a Cdc42/Rac interactive binding (CRIB) motif formed by approximately 16 residues.[11,12] As part of the GBD, the CRIB motif is usually necessary but not sufficient for a tight binding to Cdc42 and Rac1 and is participating in the regulation of the effector function.[13,14] The unstructured CRIB motif binds to the G protein and forms an intermolecular β-sheet as described for PAK1,[15] WASP,[16] and ACK1.[17]

Animals and fungi contain Cdc42, Rac, and Rho as members of the Rho family whereas plants have evolved a unique subfamily called ROPs (Rho of plants).[18] Since plants seem to lack Ras proteins, ROPs might combine the functions of Rho and Ras by controlling processes such as polar growth, pathogen defense, and stress adaption.[18,19] The presently known 11 ROPs of the model plant *Arabidopsis thaliana* are in the focus of ongoing research.[20–22] On the basis of phylogenetic analyses, four classes of ROPs can be defined, where class I contains ROP8, class II contains ROP9–ROP11, class III contains ROP7, and class IV contains ROP1–ROP6.[18,23]

As other small G proteins, ROPs are regulated by specific RopGEFs (GEFs for ROPs) and RopGAPs (GAPs for ROPs). In *A. thaliana*, 10 RopGAPs containing a RhoGAP domain of around 150 residues, including a highly conserved Arg, have been identified.[20,22] One RopGAP subfamily is characterized by a single member and contains the RhoGAP domain as the only known protein module. A second family is represented by RopGAPs with an additional Pleckstrin homology domain, implicating a possible regulation of GAP activity or localization by phosphoinositides.[1] One member called REN1 (RopGAP ROP1 enhancer 1) was recently described.[24] REN1 also contains two coiled-coil regions that bind to exocytic vesicles to regulate the RopGAP localization.

The largest RopGAP family in *A. thaliana* with six members is characterized by a CRIB motif in addition to the GAP domain.[22,25,26] In contrast, in animals and fungi, the CRIB motif has never been found in GAP proteins, only in effectors for Cdc42 and Rac1. A similar combination of these protein modules is also present in most RopGAPs of higher plants such as tobacco (*Nicotiana tabacum*),[27] rice (*Oryza sativa*), lotus (*Lotus japonicus*),[28] and grape vine (*Vitis vinifera*).[29] These RopGAPs are involved in polar cell growth and in adaptation of plants to oxygen deprivation.[27,30,31] Recently, we could show that RopGAP2 from *A. thaliana* dimerizes via its catalytic GAP domain and forms a 2:2 complex with ROP using two undistinguishable binding sites.[25] We also proposed that one ROP molecule is able to interact with both the GAP domain and the CRIB motif at the same time. Preliminary qualitative studies indicate that the CRIB motif is necessary for an efficient GAP activity and its correct subcellular localization.[26,27]

This is at least partly due to the fact that the CRIB motif is required for a high affinity and specificity in binding as recently described by us.[25] There, we have shown that the mutation or deletion of the CRIB motif leads to an up to 10-fold weaker interaction and, in addition, to the loss of the specificity in binding of RopGAP2 to ROP1, ROP7, and ROP9. For instance, RopGAP2 binds to active ROP7 with an affinity of 0.3 μM and to ROP4 with an affinity of 3.6 μM while the GAP domain shows a similar affinity towards both ROP proteins (K_d = 11.3 μM for ROP4; K_d = 30.2 μM for ROP7). Kinetic experiments demonstrate that these effects of the CRIB mutants are caused by a faster dissociation of the ROP·RopGAP complex, indicating that the CRIB motif may function as a lid for binding and/or release of ROP. Therefore, RopGAP binding and activity are obviously regulated by its CRIB motif in a novel plant-specific manner. In addition, the conserved Arg residue in the GAP domain seems to be relevant for the GAP function as shown for a tobacco CRIB-type RopGAP,[27] but its influence has not been quantified. Interestingly, our analysis also showed that the Arg residue of RopGAP2 in the presence of the CRIB motif is inhibitory for ROP binding.[25]

While the activity of mammalian RhoGAPs has been analyzed extensively, a detailed mechanistic study of the RopGAP-stimulated GTP hydrolysis of plant ROPs, as well as the comparison with the animal Rho–RhoGAP system, has not yet been performed. Moreover, very little is known about the regulatory mechanism of the RopGAP activity by its CRIB motif, while the requirement of the CRIB region for the GAP activity has been documented in qualitative studies.[26,27] It would also be interesting to know whether and how dimerization affects catalysis. Here, we present a quantitative kinetic and mutational analysis of the RopGAP2 activity from *A. thaliana* towards ROPs with focus on the regulatory role of the CRIB motif. We analyze the individual steps of the overall reaction such as complex formation, GTP cleavage, P_i release, and complex dissociation. Furthermore, we also investigate the RopGAP2 specificity towards different ROP isoforms and human Cdc42.

Results

Sequential release of two P_i molecules from the 2:2 ROP·RopGAP2 complex

As previously described, we could express and isolate a soluble and stable construct of RopGAP2 (amino acids 63–362) containing the N-terminal CRIB motif and the RopGAP domain (RopGAP2 hereinafter) and the GAP domain itself (amino acids 110–362; Fig. 1a).[25] Contrary to previous studies,[26,27] all experiments were performed with purified proteins after cleavage of the purification tag.

We analyzed the GTPase-stimulating activity of RopGAP2 towards ROP by following P_i release using the phosphate-binding protein labeled with *N*-[2-(1-maleimidyl)ethyl]-7-(diethylamino)coumarin-3-carboxamide (MDCC-PBP).[32,33] Binding of P_i to MDCC-PBP occurs tightly ($K_d \sim 0.1$ μM) and rapidly ($k_{on} = 136\ \mu M^{-1}\ s^{-1}$) and leads to an increase in MDCC fluorescence. P_i release was observed under single-turnover conditions in a stopped-flow instrument. The signal change for the reaction of ROP7·mGTP and RopGAP2 in real time is shown in Fig. 1b and c with linear and logarithmic time scales, respectively. The fluorescence traces cannot be described with a single-exponential equation (cyan, blue line) but can be fitted with two rate constants of $1.85\ s^{-1}$ and $0.17\ s^{-1}$ with similar amplitudes for both rates (red line, Tables 1 and 2). To exclude the possibility of having two protein populations, we repeated the experiments with different protein preparations at different times, which always gave the same results in terms of relative rates and amplitudes. The signal amplitude for the GAP-catalyzed reaction of 1 μM ROP7·mGTP corresponds to 1 μM P_i, suggesting the release of two P_i molecules

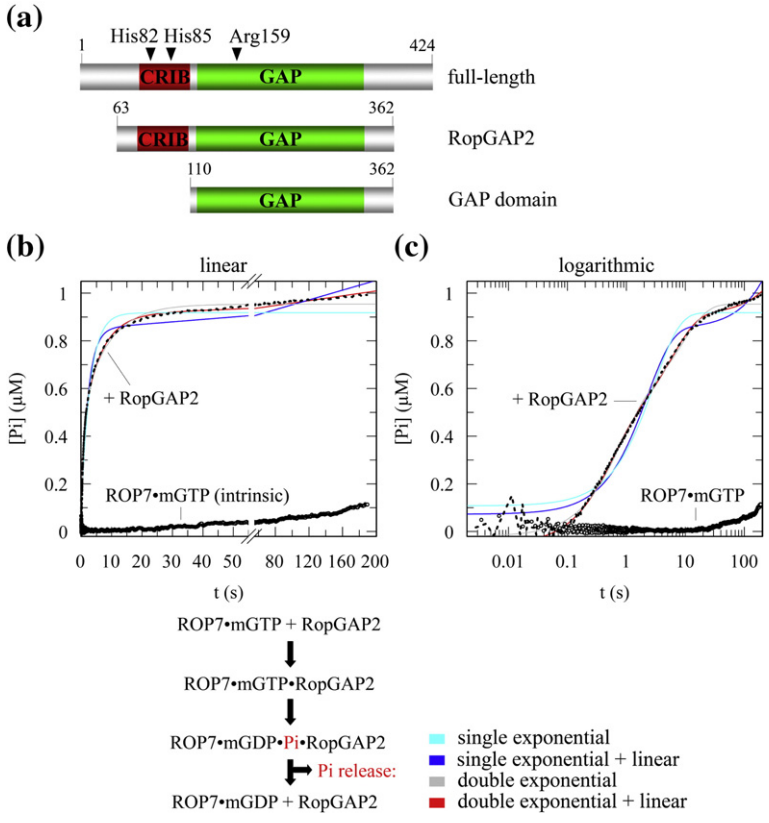

Fig. 1. RopGAP2 activity towards ROP7·mGTP measured by P_i release. (a) Schematic representation of RopGAP2 constructs from *A. thaliana* used for biochemical studies. Linear (b) and logarithmic (c) plot of single-turnover kinetics of P_i release for the RopGAP2-catalyzed (50 μM) and intrinsic GTP hydrolysis of ROP7·mGTP (1 μM) in the presence of MDCC-PBP (5 μM). MCDD fluorescence was monitored through a 455-nm-cutoff filter after excitation at 430 nm (see Materials and Methods). The GAP reaction cannot be described by a single-exponential function (cyan, blue lines) but by a double-exponential equation (red line) with a linear portion due to increasing P_i contaminations in the late phase of the reaction.

Table 1. Kinetic constants for the interaction of WT or mutant RopGAP2 with ROP4 and ROP7 bound to mGTP

	Rate constants based on mant-fluorescence changes					P_i release rates	
Protein	$k_{obs\text{-}mGTP}$ (s^{-1})	k_{int} (s^{-1})	k_{diss1} (s^{-1})	k_{diss2} (s^{-1})	$k_{obs\text{-}mGDP}$ ($\times 10^{-3}$ s^{-1})	$k_{obs1}=k_{max}$ (s^{-1})	k_{obs2} (s^{-1})
WT							
ROP4 (class IV)	5.7 ± 0.3	—	1.55 ± 0.12	0.16 ± 0.01	n.d.	—	—
ROP7 (class III)	5.5 ± 1.3	—	1.07 ± 0.23	0.14 ± 0.01	1.7 ± 0.1	1.85 ± 0.07	0.17 ± 0.01
H82A							
ROP4	6.8 ± 0.4	—	0.28 ± 0.01	0.11 ± 0.02	n.d.	—	—
ROP7	6.3 ± 0.2	—	0.23 ± 0.01	0.11 ± 0.02	1.0 ± 0.2	0.46 ± 0.02	0.16 ± 0.01
H82A–H85A							
ROP4	5.1 ± 0.2	—	—	0.37 ± 0.01	n.d.	—	—
ROP7	4.8 ± 0.3	—	—	0.23 ± 0.01	1.3 ± 0.1	0.55 ± 0.03	0.21 ± 0.01
GAP domain							
ROP4	6.3 ± 0.1	0.09 ± 0.02	—	0.02 ± 0.00	n.d.	—	—
ROP7	5.3 ± 0.1	0.12 ± 0.02	—	0.02 ± 0.01	0.8 ± 0.1	0.10 ± 0.01	0.02 ± 0.00
R159A							
ROP4	4.4 ± 0.1	1.87 ± 0.26	—	0.02 ± 0.00	2.0 ± 0.2	—	—
ROP7	4.9 ± 0.5	1.39 ± 0.10	—	0.03 ± 0.01	2.0 ± 0.1	—	0.03 ± 0.00
H82A–R159A							
ROP7	5.0 ± 0.7	0.44 ± 0.18	—	0.04 ± 0.00	1.3 ± 0.1	—	0.04 ± 0.01
GAP domain (R159A)							
ROP7	4.6 ± 0.3	0.08 ± 0.25	—	0.02 ± 0.00	n.d.	—	0.02 ± 0.01

Association and dissociation of the ROP·RopGAP complex were monitored by mant fluorescence as described in Fig. 2a and Supplemental Fig. S2 and kinetics of P_i release due to the RopGAP2 activity by MDCC fluorescence as shown in Fig. 1b and c. Data were determined with SD from three independent experiments. n.d. , not determined within the time frame.

from the 2:2 complex. The intrinsic hydrolysis reaction leads to the dissociation of only 0.1 μM P_i in the indicated time. The equation used for fitting the data contains a linear portion that describes the small signal change due to increasing P_i contaminations in the late phase of the reaction.

We performed the P_i release studies with ROP7 bound to the fluorescent-labeled mGTP to compare the P_i release rates with the kinetic constants of the complex dissociation determined in *N*-methylanthraniloyl (mant)-fluorescence experiments (see below). When we repeat the P_i release measurements under the same condition using ROP7 bound to GTP (and not to mGTP) and RopGAP2, we again observe two rates with a 10-fold difference and similar amplitudes for both rates, indicating the

Table 2. Amplitudes for the interaction of WT or mutant RopGAP2 with ROP4 and ROP7 bound to mGTP

	Signal change in mant fluorescence					P_i release	
Protein	$A_{obs\text{-}mGTP}$	A_{int}	A_{diss1}	A_{diss2}	$A_{obs\text{-}mGDP}$	A_{obs1}	A_{obs2}
WT							
ROP4 (class IV)	0.21 ± 0.02	—	0.10 ± 0.01	0.10 ± 0.01	n.d.	—	—
ROP7 (class III)	0.18 ± 0.03	—	0.07 ± 0.02	0.10 ± 0.01	0.06 ± 0.01	0.48 ± 0.05	0.49 ± 0.05
H82A							
ROP4	0.23 ± 0.03	—	0.17 ± 0.04	0.03 ± 0.01	n.d.	—	—
ROP7	0.19 ± 0.02	—	0.14 ± 0.02	0.04 ± 0.01	0.01 ± 0.00	0.42 ± 0.02	0.48 ± 0.03
H82A–H85A							
ROP4	0.21 ± 0.01	—	—	0.19 ± 0.01	n.d.	—	—
ROP7	0.16 ± 0.02	—	—	0.17 ± 0.01	0.04 ± 0.01	0.38 ± 0.01	0.55 ± 0.02
GAP domain							
ROP4	0.19 ± 0.02	0.02 ± 0.01	—	0.20 ± 0.01	n.d.	—	—
ROP7	0.16 ± 0.02	0.02 ± 0.00	—	0.20 ± 0.03	0.02 ± 0.00	0.35 ± 0.02	0.61 ± 0.05
R159A							
ROP4	0.17 ± 0.06	0.02 ± 0.00	—	0.14 ± 0.02	0.02 ± 0.00	—	—
ROP7	0.15 ± 0.03	0.02 ± 0.00	—	0.05 ± 0.01	0.03 ± 0.00	—	0.96 ± 0.03
H82A–R159A							
ROP7	0.09 ± 0.01	0.02 ± 0.00	—	0.09 ± 0.01	0.04 ± 0.00	—	0.82 ± 0.01
GAP domain (R159A)							
ROP7	0.12 ± 0.04	0.02 ± 0.01	—	0.16 ± 0.01	n.d.	—	0.96 ± 0.05

Reactions and kinetic constants are described in Figs. 1b and c and 2a, Supplemental Fig. S2, and Table 1 with SD from three independent experiments. n.d. , not determined within the time frame.

release of two P_i molecules (Supplemental Fig. S1; Supplemental Table S1). This observation demonstrates that the biphasic kinetics of P_i release is not an artifact caused by the mant group. However, the kinetic constants are 0.16 s^{-1} and 0.02 s^{-1} slower than the rates for the ROP7·mGTP reaction. This may be due to the weaker affinity of ROP7·GTP as compared to that of ROP7·mGTP such that ROP7·GTP measurement would not be performed under saturating conditions. That the mant group can affect the nucleotide affinity as well as the intrinsic and/or the GAP-mediated GTP hydrolysis has previously been demonstrated.[34,35]

Kinetics of the sequential GTPase reaction measured by mant fluorescence

The activity of RopGAP2 was also determined by monitoring GTP hydrolysis in real time with fluorescent mant-(m)GTP (Fig. 2a; Tables 1 and 2) as shown previously for the Ras–RasGAP and Arl3–RP2 interaction.[8,36] In contrast to those studies and the present experiments, no mant signal change could previously be detected for the animal Rho–RhoGAP system.[37] The interaction with the CRIB motif has been shown to produce a large fluorescence decrease on binding of Cdc42/Rac1 to animal CRIB effectors.[13,38] However, here we can observe a similar spectral change using the full-length and CRIB deletion construct of RopGAP2 (see below). The fluorescence change of the plant ROP–RopGAP reaction, however, is not simple to interpret.

The mant fluorescence change is considered to monitor association and dissociation of the ROP·RopGAP2 complex (Fig. 2a), as we could also show it in a recent article describing the complex formation.[25] Using the same single-turnover conditions as in the P_i release experiment, we were able to detect a rapid decrease in fluorescence with a single rate $k_{obs\text{-}mGTP}$ of 5.5 s^{-1}, representing binding of

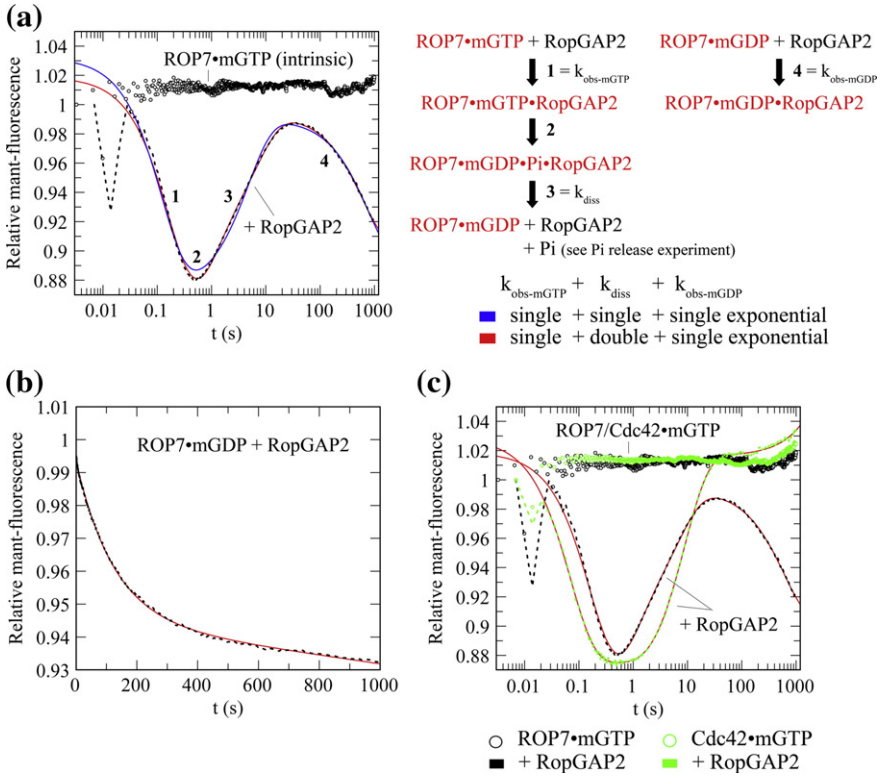

Fig. 2. RopGAP2 activity towards plant ROPs and human Cdc42 observed with mant fluorescence. (a) Monitoring of the RopGAP2 (50 μM) activity towards ROP7·mGTP (1 μM) by mant fluorescence under the same conditions as in Fig. 1b and c but without MDCC-PBP. Mant fluorescence was detected through a 408-nm-cutoff filter after excitation at 360 nm. RopGAP2 binding to ROP7·mGTP leads to a fluorescence decrease, followed by an increase due to GTP hydrolysis and complex dissociation (see scheme of the partial reaction steps). The second decrease in fluorescence is caused by rebinding of ROP7·mGDP. Data of the GAP reaction can be described by a quadruple-exponential function (red line, Tables 1 and 2), not by a triple-exponential fit (blue line). (b) Association of RopGAP2 (50 μM) and ROP7·mGDP (1 μM) observed by mant fluorescence. Data can be fitted by a monoexponential equation with a linear portion (red line). (c) Monitoring of the RopGAP2 activity towards Cdc42·mGTP by mant fluorescence as described for the ROP7·mGTP interaction in (a); ROP7 data are also shown (in black). The GAP reaction of Cdc42·mGTP can be fitted by a triple-exponential function with a linear portion (red line, Table 3).

ROP7·mGTP and RopGAP2 (Table 1). Upon GTP hydrolysis, dissociation of RopGAP2 from the weakly binding product ROP·mGDP is measured by an increase in fluorescence with a similar amplitude as for the fluorescence decrease (Fig. 2a; Table 2). As in the P_i release experiment, the dissociation of products also has to be described by two rate constants, $k_{diss1} = 1.07\ s^{-1}$ and $k_{diss2} = 0.14\ s^{-1}$, similar to the rate constants observed for P_i release (Table 1). Moreover, the amplitudes for the fast and the slow rate have the same size, as in the P_i release measurement (Table 2).

Both the kinetics of P_i release and mant fluorescence support a nearly complete GAP-catalyzed hydrolysis reaction and ROP·mGDP release after 40 s (Figs. 1b and c and 2a). Quite unexpectedly, we observe another fluorescence decrease after 40 s with a rate constant $k_{obs\text{-}mGDP}$ of $1.7 \times 10^{-3}\ s^{-1}$ (Fig. 2a; Table 1). We assign this rate, which is 3300-fold slower than the association with ROP7·mGTP, to the re-association of ROP7·mGDP and RopGAP2. Control experiments with comparable concentrations of ROP7·mGDP and RopGAP2 indeed show a fluorescence decrease, indicating association with a similar amplitude, although the rate is somewhat faster with $8.1 \times 10^{-3}\ s^{-1}$ when starting from isolated components (Fig. 2b). Long-time fluorescence measurements with the same concentration of ROP·mGTP confirm that ROP is stable under these conditions and the decrease in fluorescence is not due to mant-nucleotide release (data not shown).

The change in mant fluorescence for the entire ROP–RopGAP2 interaction can be fitted very well with a quadruple-exponential function (red line, Fig. 2a) describing a monophasic association of ROP7·mGTP (decrease in fluorescence), a biphasic dissociation of products due to RopGAP activity (increase in the signal), and a monophasic re-binding of ROP7·mGDP (decrease in the signal). Describing the increase in mant fluorescence and therefore the product dissociation with a single-exponential function leads to significant deviations of the fit as shown in Fig. 2a (blue line).

In summary, we determine similar rates for P_i release and product dissociation of the RopGAP2 reaction. The ratio of the amplitudes between the fast and the slow reaction is comparable in both types of activity experiments. The mant fluorescence data can be described very well by the equation used and show no indication for the accumulation of a P_i-bound intermediate (Fig. 2a). Moreover, we do not observe a lag phase in the P_i release data (Fig. 1b and c). The absence of any observable accumulation of a P_i-bound intermediate allows us to conclude that the P_i release rate is in the same range (less than 10-fold difference) than the chemical GTP cleavage step. These data do not allow us to make any conclusion about the rate of the GTP cleavage since we could not directly measure it. This is unlike the case for the Ras–RasGAP and the Rap–RapGAP interactions where P_i release is rate-limiting as previously shown by Fourier transform infrared measurements.[39–42]

Here, we consider the rate constants for P_i release (and, in principle, for the complex dissociation) as GTP hydrolysis rates of the two active sites in the 2:2 ROP·RopGAP complex. The active sites are different in terms of their GTPase activity, with reaction rates showing a 10-fold difference. This corresponds to a 7000-fold and 640-fold acceleration of the intrinsic ROP7·GTP hydrolysis of $2.7 \times 10^{-4}\ s^{-1}$, as determined in HPLC experiments (data not shown). To our knowledge, the ROP–RopGAP2 complex is the first GAP complex that shows a sequential GTP hydrolysis. The faster rate constant k_{obs1} of $1.85\ s^{-1}$ is in a similar range as determined for animal RhoGAPs and other GAPs, while k_{obs2} is 10-fold slower.[8,10,34,36]

RopGAP2 shows specificity in binding but not in its activity towards different ROPs

We have recently demonstrated that RopGAP2 binds with a 10-fold higher affinity to active ROP7 ($K_d = 0.3\ \mu M$) than to ROP2, ROP3, and ROP4 ($K_d = 3.6$–$4.7\ \mu M$).[25] Therefore, we wondered whether RopGAP2 shows specificity in its GAP activity towards different ROP isoforms. As described for ROP7·mGTP (see above), we also analyzed the RopGAP2 activity towards ROP2, ROP3, and ROP4 under single-turnover conditions in stopped-flow experiments. Following mant fluorescence, we observe a sequential release mechanism and obtain similar kinetic constants and amplitudes for all tested ROP isoforms (Table 3). GTP hydrolysis rate constants are represented by the rates of the complex dissociation k_{diss1} and k_{diss2} because P_i release was not determined. Under the conditions used, RopGAP2 shows no specificity in its stimulation of the intrinsic GTP hydrolysis for ROP2, ROP3, ROP4, and ROP7 (7000- to 9600-fold for k_{diss1} and 640- to 950-fold for k_{diss2}) which does not correlate with the observed binding specificity.[25]

To make sure that we are working under saturating conditions, we varied the GAP concentration for the reaction of ROP4·mGTP. As expected, with increasing concentrations of RopGAP2, we measure a faster association of the complex ($k_{obs\text{-}mGTP}$) and an increase in the amplitude (Fig. 3a and b). While the second hydrolysis reaction (indirectly determined as k_{diss2}) is saturated at around 10 μM, the faster hydrolysis step (k_{diss1}) increases up to the highest GAP concentration tested, with a 10-fold difference between the consecutive reactions. Since the reaction with the tighter-binding ROP7 isoform is clearly saturated at 50 μM (data not shown), k_{diss1} only slightly increases in the 10- to 50-μM range and the rates

Table 3. The interaction of RopGAP2 with different plant ROPs and human Cdc42 bound to mGTP

	Kinetic constants				
Protein	$k_{obs\text{-}mGTP}$ (s^{-1})	k_{int} (s^{-1})	$k_{diss1}=k_{max}$ (s^{-1})	k_{diss2} (s^{-1})	$k_{obs\text{-}mGDP}$ ($\times 10^{-3}$ s^{-1})
ROP2 (class IV, At)	5.8 ± 1.2	—	1.90 ± 0.34	0.18 ± 0.04	2.0 ± 0.1
ROP3	5.3 ± 0.1	—	2.00 ± 0.13	0.17 ± 0.01	n.d.
ROP4	5.7 ± 0.3	—	1.55 ± 0.12	0.16 ± 0.01	n.d.
ROP7 (class III, At)	5.5 ± 1.3	—	1.07 ± 0.23	0.14 ± 0.01	1.7 ± 0.1
Cdc42 (Hs)	14.3 ± 0.8	1.11 ± 0.1	—	0.11 ± 0.01	—
	Amplitudes				
Protein	$A_{obs\text{-}mGTP}$	A_{int}	A_{diss1}	A_{diss2}	$A_{obs\text{-}mGDP}$
ROP2 (class IV, At)	0.21 ± 0.04	—	0.11 ± 0.03	0.09 ± 0.02	0.02 ± 0.00
ROP3	0.22 ± 0.02	—	0.13 ± 0.02	0.09 ± 0.01	n.d.
ROP4	0.21 ± 0.02	—	0.10 ± 0.01	0.10 ± 0.01	n.d.
ROP7 (class III, At)	0.18 ± 0.03	—	0.07 ± 0.02	0.10 ± 0.01	0.06 ± 0.01
Cdc42 (Hs)	0.15 ± 0.04	0.03 ± 0.01	—	0.17 ± 0.03	—

Experiments were performed as shown in Fig. 2a with SD from three independent measurements. n.d. , not determined. At , *A. thaliana*; Hs , *Homo sapiens*.

for ROP4 and ROP7 are very similar at 50 μM (Table 3), we assume that we are working under saturated conditions in both cases. Due to the 10-fold lower affinity of ROP4·mGppNHp as compared to ROP7·GppNHp [GppNHp being guanosine 5′-(β,γ-imido)triphosphate],[25] and assuming the same tendency for the GDP conformation, no re-binding can be observed for ROP4 (Fig. 3).

The CRIB motif is necessary for an efficient GAP activity and sequential ROP·GDP release

The CRIB motif of RopGAP2 is highly homologous to the CRIB region in the plant ROP effectors RICs (ROP-interacting CRIB-motif-containing proteins) with 47% sequence identity and to human Cdc42/Rac1 effectors such as WASP with 41% sequence identity.[25] To analyze the influence of the CRIB motif on the RopGAP2 activity, we mutated one or both of its conserved His residues (His82 and His85) to Ala or deleted the motif entirely (GAP domain construct, Fig. 1a). Previous studies demonstrated that these His residues in plant RopGAP2 and in animal CRIB effectors are required for a tight and specific binding to the cognate G protein.[15,25,43,44]

When we measure P_i release from ROP7·mGTP in the presence of the single- and the double-His mutant, we still observe a sequential GTP hydrolysis and release of two P_i molecules as for the wild-type (WT) protein (Fig. 4; Tables 1 and 2). However, the fast reaction rate k_{max} for both mutants is reduced 4-fold compared to the WT protein while release of

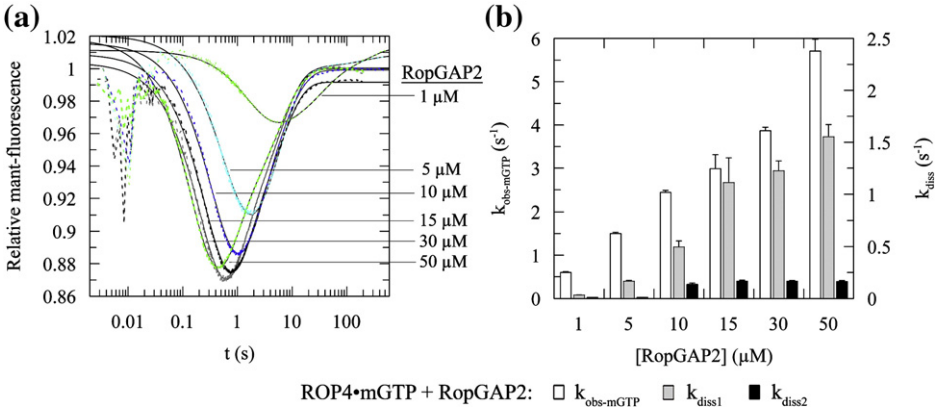

Fig. 3. Catalysis of the ROP4·mGTP hydrolysis and its dependence on RopGAP2 concentration. (a) Stimulation of the ROP4·mGTP hydrolysis (1 μM) with increasing RopGAP2 concentrations (1–50 μM), observed through mant fluorescence as described in Fig. 2a. A scheme of the individual reaction steps is shown in Fig. 2a. The data can be fitted by a triple-exponential function. (b) Apparent kinetic constants for association ($k_{obs\text{-}mGTP}$, left axis) and dissociation (k_{diss}, right axis) between ROP4·mGTP and the indicated RopGAP2 concentrations. Error bars are the mean ± SD from three independent measurements.

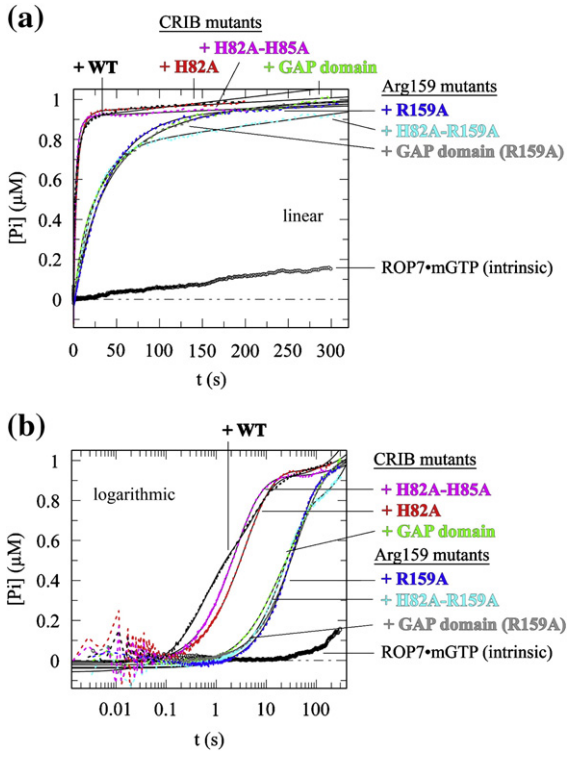

Fig. 4. Effects of the CRIB motif and the conserved Arg159 on P_i release. Stopped-flow kinetics of P_i release for the intrinsic and the WT or mutant RopGAP2-catalyzed GTP hydrolysis of ROP7·mGTP in the presence of MDCC-PBP as described in Fig. 1b and c, presented with a linear (a) and a logarithmic (b) time scale. Data of GAP reactions can be fitted by a single- or double-exponential equation (thin line, Tables 1 and 2) with a linear portion caused by increasing P_i contaminations within the time frame.

the second P_i molecule is very similar to that of RopGAP2(WT). Overall, the difference between k_{max} (k_{obs1}) and k_{obs2} is only 3-fold for both His mutants, but the amplitudes of the two rates are in the same range as that of RopGAP2(WT) (Tables 1 and 2). When we monitor the reaction with ROP7·mGTP via mant fluorescence as probe, formation of the complex with the H82A mutant as described by $k_{obs\text{-}mGTP}$ is not affected (Fig. 5a; Table 1), and it shows a sequential release of ROP7·mGDP (k_{diss}). The two rates are 0.23 s^{-1} and 0.11 s^{-1} for the first and the second reaction, respectively, and the 2-fold difference is similar as in the P_i release assay. The H82A–H85A mutation does not affect the rate of complex formation either, but the fluorescence increase (release of the products) can now be fitted with a single-exponential equation, while the amplitude of the signal corresponds to the sum of those for the WT protein (Tables 1 and 2). The release rate (k_{diss2}) is similar to the rate of the second P_i release (k_{obs2}) and in the same range as k_{diss2} of RopGAP2(WT).

When we delete the CRIB motif and monitor the reaction of the GAP domain by P_i release, we again find two sequential reactions with the same overall amplitude (i.e., two molecules of P_i released) as for the WT protein (Fig. 4; Tables 1 and 2). These observations suggest that the CRIB motif is, in principle, not required for a sequential GTP hydrolysis. However, the rate constants for both steps are significantly decreased to 0.10 s^{-1} (19-fold) and 0.02 s^{-1} (9-fold). The difference between the rates is 5-fold, somewhat higher than that for His mutants. Measuring the GAP reaction with mant fluorescence (Fig. 5a) shows that the complex association is not perturbed, but dissociation of the product ROP·mGDP following the chemical step is very slow and, as in the double-His mutant, can be described by a single rate constant that is identical with the second P_i release rate k_{obs2} (Table 1). The overall amplitude corresponds to the total signal of the WT protein (Table 2). In summary, these results

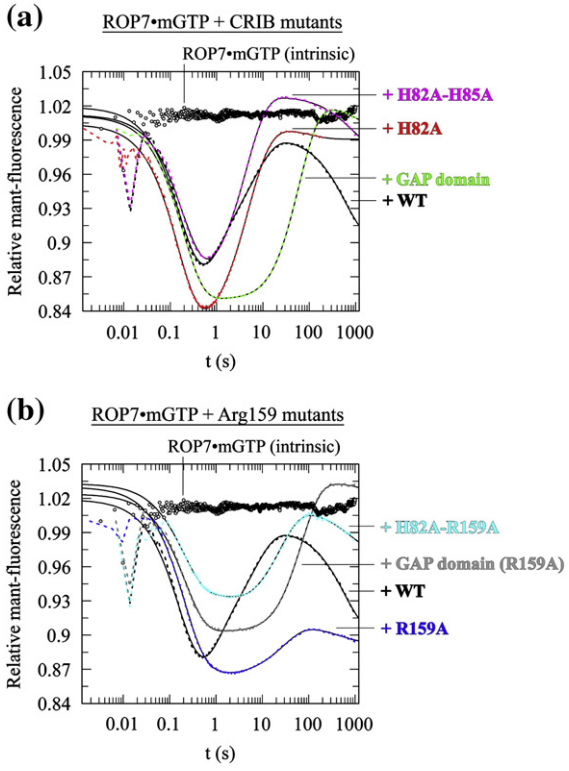

Fig. 5. Influence of the CRIB motif and the conserved Arg159 on the RopGAP2 activity measured with mant fluorescence. Monitoring complex association and dissociation and, indirectly, the GTP hydrolysis reaction through mant fluorescence using ROP7·mGTP and RopGAP2(WT) or CRIB mutants (a) or Arg mutants (b) as described in Fig. 2a. Data of GAP reactions can be fitted by a triple- or quadruple-exponential function (Tables 1 and 2).

indicate that both the mutation and the deletion of the CRIB motif slow down the RopGAP reaction and that P_i is released after or with GTP cleavage in the first active site while, unlike in the WT situation, ROP·mGDP remains bound and dissociates together with the second ROP·mGDP after or with the second P_i release.

Deletion of the CRIB motif has another dramatic effect in that it leads to an accumulation of an intermediate represented by an expanded minimum with a rate constant, denoted k_{int}, of 0.12 s^{-1} and a small amplitude of 0.02 (10% of the total signal, Tables 1 and 2). This rate can be clearly correlated with GTP cleavage as it is identical with the first cleavage reaction measured as P_i release (Table 1).

Finally, re-binding of ROP7·mGDP to RopGAP seems to occur in all CRIB mutants (Fig. 5a; Table 1). Due to the slower GAP activity and the weaker affinity of the CRIB mutants (reduced 13-fold for the His mutants and 100-fold for the GAP domain)[25] to ROP7·GTP and probably also to the GDP-bound conformation, the amplitude of the re-binding step detected within the time frame of the experiment is smaller than that for the WT protein (Table 2). Based on these experiments and those obtained with ROP4 (Supplemental Fig. S2), we can assume a role of the CRIB region also for the re-binding step.

As mentioned above, RopGAP2(WT) shows no preference in activity towards different ROP isoforms (Table 3). The same effect can be observed for all CRIB mutants since we determined similar rate constants and amplitudes for the reaction with ROP4·mGTP as with ROP7·mGTP (Tables 1 and 2; Supplemental Fig. S2).

The catalytic Arg159 is required for an efficient GTP hydrolysis and sequential release of P_i and ROP·GDP

A qualitative study of a CRIB-type RopGAP from tobacco had indicated that the highly conserved Arg in the GAP domain is crucial for the GAP activity.[27] To quantify the role of the invariant Arg159 in the GAP domain of RopGAP2 and its effect on the sequential GTP hydrolysis reaction, we introduced the R159A mutation into intact, mutated, and deleted CRIB region proteins. The GAP activity of these Arg mutants towards ROP7·mGTP measured by P_i release shows similar signal amplitudes as for RopGAP2(WT), indicative of two equivalents of P_i release (Fig. 4; Table 2). Unexpectedly, the time course of P_i release can clearly be described by single-exponential function (Table 1), suggesting that both P_i molecules are released with very similar or identical rates independently from each other. In addition to the stoichiometry of the P_i release study, gel permeation chromatography experiments illustrated that the R159A mutant preserves the ability to form a 2:2 complex.[25]

As expected for the function of the Arg159 as a catalytic residue, the rate of P_i release is down to 0.03 s^{-1} for RopGAP2(R159A), a 62- and 6-fold reduction in k_{max} and k_{obs2}, respectively. The effect of the Arg finger mutation in human RhoGAP is only slightly stronger.[34] An additional H82A mutation or deletion of the CRIB motif in the R159A background does not decrease the single-exponential rate of P_i release any further (Table 1). Furthermore, the dissociation of ROP·mGDP from the active site as monitored through mant fluorescence (Fig. 5b) follows the same rate constant as the P_i release for all Arg mutants (Table 1). Taken together, mutation of Arg159 has three effects: it reduces the efficiency of GAP catalysis, suppresses the effect of the CRIB motif, and obliterates the difference between the two active sites, as shown by both P_i release and mant-fluorescence experiments.

As described for RopGAP2(WT) (see above), the Arg mutants show re-binding of ROP·mGDP, but the effect is less apparent due to the slow fluorescence increase during k_{diss2} (Fig. 5b; Tables 1 and 2; Supplemental Fig. S2). In the case of RopGAP2 (R159A) and ROP7, we observe only a partial increase in mant fluorescence after hydrolysis, while the P_i release measurements show similar kinetics and stoichiometry (Tables 1 and 2). This suggests that only part of the ROP7·mGDP product is released and/or that ROP7·mGDP dissociation and re-association are much faster, as a result of the higher affinity of the R159A mutant.[25] For RopGAP2 (H82A–R159A), we detect a signal change of only 6% for $k_{obs\text{-}mGTP}$ and k_{diss} instead of approximately 14% as observed for the WT protein and most of the other RopGAP2 mutants (Fig. 5b; Table 2), which is not due to incomplete saturation as suggested from the affinity measurements.[25]

Both types of activity studies demonstrate that mutation of the invariant Arg159 leads to a catalytic defect and to loss of the sequential release for both P_i and ROP·mGDP. We thus suppose that the cleavage step itself is likewise disturbed, as can be assumed from previous mutational studies of Arg fingers in RhoGAP and other animal GAPs.[6–8,34,36] We interpret our data such that catalysis and product release in the first active site are slowed down enough that they are not any longer rate-limiting for the catalysis in the second site.

In mant fluorescence experiments with ROP·mGTP and the R159A mutants, we observe an accumulation of a low-amplitude intermediate with the rate constant k_{int} (Fig. 5b; Tables 1 and 2; Supplemental Fig. S2). For ROP7·mGTP, these rates are 1.39 s^{-1}, 0.44 s^{-1}, and 0.08 s^{-1} for the Arg mutants in WT, H82A, and GAP domain background, respectively, and thus very close to the first P_i release rates of the corresponding proteins without the R159 mutation. Since it has to be assumed that the Arg mutation

significantly reduces the rate of the chemical step, we assign the intermediate to a pre-hydrolysis step with a very low amplitude change (0.02 for every mutant, Table 2). We assume that in the presence of Arg159, this pre-hydrolysis step coincides with the first hydrolysis reaction, while in the absence of Arg159, both the first and the second cleavage reactions are much slower such that the formation of the intermediate can thus be detected.

RopGAP2 shows an impaired GAP activity towards human Cdc42

ROPs share at least 40% identical amino acids with animal Rho proteins.[20] As we recently reported,[25] RopGAP2 shows a comparable affinity to human Cdc42 and plant ROPs in their triphosphate state. For that reason, we also determined the RopGAP2 activity towards Cdc42·mGTP as described for ROP7·mGTP (see above). The total fluorescence change of the RopGAP reaction with both Cdc42·mGTP and ROP7·mGTP is similar (Fig. 2c). The data of Cdc42 can be described by a triple-exponential equation and those of ROP7 can be described by a quadruple-exponential function (Table 3). The decrease in fluorescence describes the binding reaction of Cdc42·mGTP and RopGAP2 with a 3-fold faster $k_{obs\text{-}mGTP}$ rate of 14.3 s^{-1} than that for ROP7. As for the reaction of ROP·mGTP with the GAP domain or the Arg mutants, a second rate k_{int} with a similar small amplitude of 0.03 is assigned to the decrease in the mant signal. This is also interpreted as the accumulation of an intermediate with k_{int} of 1.11 s^{-1}. This is most likely the GTP hydrolysis reaction itself, of either one or both Cdc42 molecules, or a conformational change preceding it. The fluorescence increase describing the dissociation of products due to the RopGAP2 activity is determined as a single rate (k_{diss2}) of 0.11 s^{-1}, which is equal to k_{diss2} of the ROP interaction. In contrast to the latter, we do not observe a second decrease in fluorescence for Cdc42, which would describe the re-binding reaction of Cdc42·mGDP and RopGAP2 (Fig. 2c). The increase in the mant signal detected after 150 s is likely due to protein aggregation.

P_i release experiments could not be performed due to technical reasons during the nucleotide exchange procedure, resulting in P_i contaminations (see Materials and Methods). The result of the mant experiment indicates an impaired RopGAP activity towards human Cdc42, although we cannot clearly assign the measured rate constant to any of the steps during GTP hydrolysis. However, based on k_{int} and k_{diss2}, RopGAP2 shows a 61-fold and a 617-fold acceleration in the intrinsic Cdc42·GTP hydrolysis (1.8×10^{-3} s^{-1} determined in HPLC experiments, data not shown), respectively, which are both slower than k_{max} of the ROP–RopGAP2 reaction.

Discussion

The largest RopGAP family from higher plants such as *A. thaliana* contains the plant-specific combination of a RhoGAP domain and a CRIB motif.[22] Here, we show that RopGAP2 is likely to use a similar chemical mechanism for the cleavage reaction as animal RhoGAPs,[4–8] confirming previous assumptions.[22,25,27] The RopGAP2 domain contains a catalytic Arg finger, and ROPs have a conserved Gln residue in the switch II region that coordinates the attacking water as known for animal Rho proteins. Furthermore, RopGAPs form a high-affinity complex with ROP·GDP only in the presence of aluminum fluoride (AlFx) to mimic the transition state of the GTP hydrolysis[25,26] as documented for non-plant GAPs.[45] Moreover, RopGAPs from *A. thaliana* show cross-activity towards human Cdc42 although it is somewhat lower as demonstrated in this and a previous study.[26] The CRIB-type RopGAP from tobacco shows no loss of GAP activity towards human Rac1 as compared to plant ROP.[27]

We recently described that one ROP molecule is able to bind simultaneously to the CRIB motif via its β2 and α5 region and to the RopGAP domain mainly via the P-loop and the switch regions, as deduced from a homology model (Fig. 6a).[25] The model, which is based on the structure of the Rho·RhoGAP complex superimposed on ROP4·GDP and the Cdc42·WASP-CRIB complex, also demonstrates that the CRIB motif is close to the active site in the ROP·RopGAP complex and may function as a component of the active site. The CRIB motif of RopGAP2 mediates high affinity and specificity in binding to ROP[25] and both the CRIB region and the RopGAP2 domain are required for an efficient GAP activity (this study and Refs. 26 and 27), which is likely to be similar to the contacts in Rho–RhoGAP and Rho–effector complexes. Since the CRIB motif in animal effectors has been shown to be unstructured and is involved in intra-steric inhibitory contacts,[15–17] we postulate an interaction between the CRIB motif and the GAP domain similar to WASP.[25] Based on the extremely slow association rate constant and the effect of CRIB mutations as previously described,[25] we suggest that this interaction has to be relieved in order for ROP to be able to bind and the CRIB region to become structured.

RopGAP2 dimerizes via its GAP domain and forms a 2:2 complex with ROP (Fig. 6b).[25] Both ROP·GTP molecules seem to bind to RopGAP2 independently from each other with very similar rates.[25] Therefore, the binding sites are likely to be identical and the asymmetry in terms of catalytic efficiency develops in the steps following the initial binding reaction. Following binding, we envision an accommodation step whereby the machinery of one active site is assembled, including positioning of the

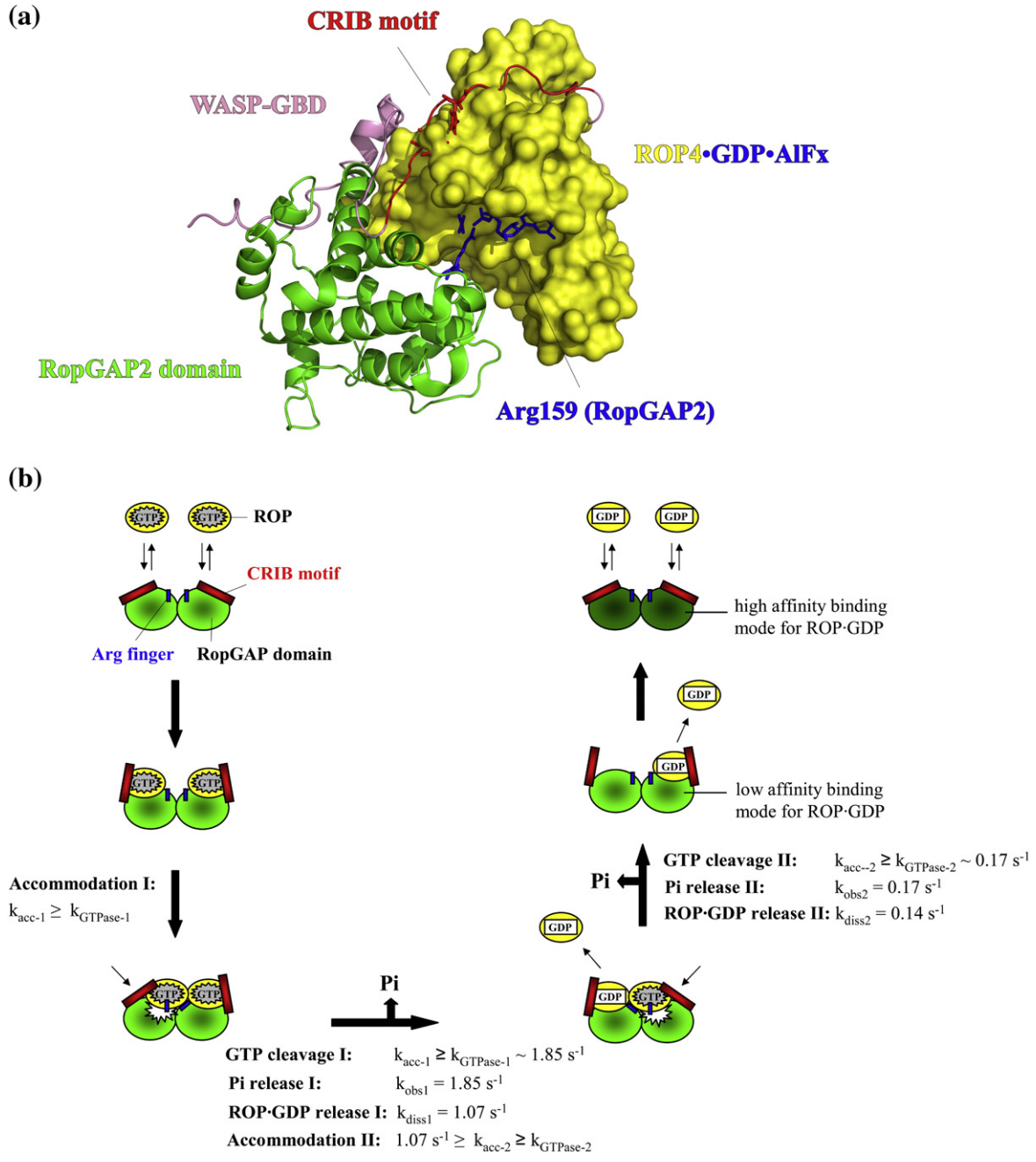

Fig. 6. A model for the ROP–RopGAP2 interaction. (a) Homology model of the ROP·RopGAP complex (color coding as indicated). The model of the monomeric RopGAP2 domain from *A. thaliana* is based on the structure of the human RhoGAP domain [Protein Data Bank (PDB) ID: 1tx4] and sequence alignment of both GAP domains (www.sbg.bio.ic.ac.uk/3dpssm). The complex structure of ROP4 (in surface representation, from ROP4·GDP·Prone8, PDB ID: 2nty) and the RopGAP2 domain was obtained by superimposition onto the structure of the RhoA·GDP·AlFx·RhoGAP complex (PDB ID: 1tx4). Through an overlay of ROP4 and Cdc42 (from Cdc42·GppCH2p·WASP-GBD, PDB ID: 1cee), the position of the CRIB motif from human WASP-GBP was defined. The conserved His residues of the CRIB region are represented by red sticks; the catalytic Arg159 of the RopGAP domain, GDP, and AlFx are shown in blue. (b) Schematic model of the proposed sequential GTP hydrolysis mechanism for the RopGAP-catalyzed GTP hydrolysis of ROP as discussed in the text. Kinetic constants were determined for the interaction of ROP7 and RopGAP2 (k_{acc}, rate of accommodation; k_{GTPase}, rate of GTP cleavage; k_{obs} and k_{diss} see Table 1).

catalytic Arg159 (Fig. 6b). Accommodation cannot be observed in RopGAP2(WT) where the GTP cleavage, P_i release, and dissociation of ROP·GDP are very fast, at least for the first cleavage step. It is, however, visible as an additional kinetic step with low fluorescence amplitude in some of the mutants such as the R159A mutants where the following cleavage is much slower. A similar pre-hydrolysis rate-limiting conformational step has been observed for the Ras–RasGAP reaction, where the movement of the Arg finger into the active site determines the rate of the GTP cleavage reaction.[46] For the ROP–RopGAP2 interaction, the rate k_{diss1} is linearly dependent on the GAP concentration up to 50 μM, whereas k_{diss2} is already saturated at 10 μM. Although the data do not allow assigning the second rate to a particular reaction step in the second active site, we would like to assign it to the accommodation step for the second site (Fig. 6b). For the animal Rho–RhoGAP system, structural analysis has shown that the active site including the Arg finger needs to be assembled for catalysis to happen.[5,47]

Although we have no structural model of the RopGAP2 dimer interface, we assume that dimerization somehow brings both active sites into close proximity such that the two active sites cannot assemble independently anymore and that accommodation can only occur in one active site and thus creates asymmetry (Fig. 6b). This steric interference is apparently dependent on the Arg finger and the CRIB motif, which we think acts as a lid for binding and/or release of ROP.[25] We conclude that hydrolysis takes place in both active sites independently from each other and that accommodation of the second site can only occur after the first ROP·GTP has been cleaved and the product ROP·GDP has been released. The k_{max} of RopGAP2(WT) is in the same range as described for other animal GAPs, as the effect of the Arg mutation on catalysis.[8,34,36]

Since no intermediates for each of the two hydrolysis reactions could be detected, the conclusion that P_i release is in the same range (less than 10-fold rate difference) as GTP cleavage can be drawn. In order for the second site to become GTPase competent, ROP·GDP has to be released with a similar rate as P_i, which is another indication that two ROP molecules prevent simultaneous accommodation of the active sites. After the second GTP hydrolysis and dissociation of products, ROP·GDP can re-bind to RopGAP. Re-binding is only observed in cases where affinity to a particular ROP isoform or mutant is high, such as with ROP7 as compared to ROP4 with a 10-fold lower affinity.[25] Since both ROP·GDP molecules dissociate after the GTP hydrolysis before re-binding occurs (in the WT protein), one has to assume a conformational change from a low-affinity binding site for ROP·GDP after the GTP hydrolysis to a high-affinity site for re-binding. For the transition to the latter one, the CRIB motif seems to be relevant.

In the 2:2 complex, RopGAP2 stimulates the ROP·GTP hydrolysis in a sequential manner with a 10-fold difference between both hydrolysis reactions (Fig. 6b). From stopped-flow experiments, we cannot decide whether or not the actual GTP cleavage reactions are sequential since we only observe release of the products P_i and ROP·GDP from the complex, but not their actual generation. Preliminary Fourier transform infrared measurements seem to suggest that the actual cleavage reaction is sequential as well (Kötting *et al.*, unpublished data). The sequential reaction monitored by P_i release becomes much less pronounced with the CRIB mutants. The release of products as measured by mant fluorescence is finally described by a single rate constant for the CRIB double and the deletion mutant. This indicates that, in this case, ROP·GDP does not have to dissociate from the complex in order for the second reaction to take place and that both ROP·GDP molecules are released after the second GTP cleavage reaction. For the Arg finger mutants, GTP hydrolysis is probably not sequential anymore and both P_i and ROP·GDP dissociation are described with one and the same rate.

The reaction between plant ROP and RopGAP2 is the first described GAP interaction showing sequential GTP hydrolysis reactions. This type of nucleotide hydrolysis reaction has previously been observed in animal and bacterial ABC transporters. These proteins dimerize in an ATP-dependent manner to provide the membrane transport of many substrates.[48] The ATP hydrolysis reactions in both active sites show a similar activity difference as observed for RopGAP2.[49,50] In this case, the sequential reaction is based on a different arrangement of the catalytic machinery in both active sites and not due to the vicinity of the active sites as proposed in our model for the plant RopGAP2 protein. Until today, the biological relevance of a sequential hydrolysis of ABC transporters is not obvious either.

To find out whether dimerization of RopGAP2 is necessary for an efficient GAP activity and to confirm our model, we mutated residues in several different regions of the GAP domain model chosen for being surface exposed and plant specific (data not shown). However, none of these affected dimerization. An important step to answering these questions would require the determination of the 3D structure of the ROP·RopGAP complex, which we have not been able to achieve. Interestingly, activation of ROP through the receptor kinases–GEF reaction is also mediated by dimeric interaction modules, suggesting that the GAP-catalyzed inactivation by a dimeric regulator follows the same principle and is biologically significant.[25]

Materials and Methods

Constructs and protein purification

Cloning of RopGAP2 (residues 63–362), the GAP domain (residues 110–362), ROP2 (residues 1–179), and ROP3, ROP4, and ROP7 (residues 1–180) was described previously.[25] Site-specific mutagenesis was performed via the QuikChange method (Stratagene). Expression of all proteins as glutathione *S*-transferase fusion proteins in *Escherichia coli* BL21 Codon Plus(DE3)RIL (Stratagene) and the purification (including cleavage of the glutathione *S*-transferase tag) were described previously.[25]

Nucleotide exchange and preparation of nucleotide-free protein

For P_i release experiments, nucleotide exchange of ROP·GDP to mGTP was performed with 25 mM ethylenediaminetetraacetic acid and a 9-fold molar excess of mGTP overnight at 4 °C. ROP was then purified by an S75 column in buffer A (50 mM Hepes, pH 7.7, 100 mM NaCl, 5 mM $MgCl_2$, 5% glycerol, and 5 mM β-mercaptoethanol). mGTP loading was calculated by determining the concentration of ROP and the nucleotide.

For mGDP and mGTP stopped-flow studies, ROP/Cdc42·GDP was at first loaded with $GppCH_2p$ by incubation with alkaline phosphatase (1 U/mg protein; rAPid, Roche) overnight at 4 °C and a 1.5-fold molar excess of $GppCH_2p$. After GDP degradation was monitored via HPLC, the G protein was purified by using an S75 column in buffer A, flash frozen in liquid nitrogen, and stored at −80 °C. For exchange to mGDP, ROP·$GppCH_2p$ was incubated with phosphodiesterase (2.5 U/mg protein; Sigma-Aldrich) and a 1.5-fold molar excess of mGDP at 4 °C until degradation of $GppCH_2p$, measured by HPLC. Three cycles of shock-freezing in liquid nitrogen and thawing inactivated the phosphodiesterase. The G protein was purified and stored as described above. For preparation of the nucleotide-free form, ROP/Cdc42·$GppCH_2p$ was treated in the same way but without adding mGDP and a gel permeation chromatography.

HPLC measurements

HPLC experiments were performed as described previously to determine the nucleotide state of the G protein and to measure the intrinsic GTP hydrolysis of ROP·GTP.[25]

Measurement of P_i release

P_i release was measured as described previously,[32,33] using fluorescence change of the A197C mutant of the phosphate-binding protein from *E. coli* labeled with MDCC. Before the measurements, the stopped-flow instrument (SX18-MV, Applied Photophysics) was incubated for 20 min at 20 °C with 200 μM 7-methylguanosine and 1 U/ml purine nucleoside phosphorylase to minimize P_i contamination. For the experiments, 1 μM ROP·(m)GTP and 50 μM WT or mutant RopGAP2 were mixed in the presence of 5 μM MDCC-PBP (final concentrations in the mixing chamber) in buffer A at 15 °C. MDCC fluorescence was monitored through a 455-nm-cutoff filter after excitation at 430 nm. P_i concentration was calculated from fluorescence change, normalized to the P_i concentration of a standard curve. At least five kinetic measurements were performed under identical conditions, averaged, and fitted by nonlinear regression to determine the apparent rate constants k_{obs}, using Grafit (Erithacus Software).

Stopped-flow kinetics monitoring by mant fluorescence

All experiments were performed in buffer A at 15 °C in a stopped-flow instrument. The change in mant fluorescence was observed through a 408-nm-cutoff filter after excitation at 360 nm. At least five kinetic measurements were performed under identical conditions, averaged, and analyzed by nonlinear regression as described for P_i release experiments. To monitor complex association and dissociation due to the RopGAP activity, we mixed 1 μM ROP/Cdc42·mGTP and 50 μM WT or mutant RopGAP2 (final concentrations). Before the measurement, 1.5 μM nucleotide-free ROP/Cdc42 was pre-incubated with 1 μM mGTP on ice. Formation of the mGDP complex was analyzed by mixing 1 μM ROP7·mGDP and 50 μM RopGAP2(WT).

Modeling

Superimpositions and figures were prepared with PyMOL (DeLano Scientific†).

Supplementary materials related to this article can be found online at doi:10.1016/j.jmb.2011.06.033

Acknowledgements

A. Schaefer and A. Berken were supported by the Priority Program SPP1150 of the Deutsche Forschungsgemeinschaft; M. Miertzschke was supported by the SFB 642 of the Deutsche Forschungsgemeinschaft. We thank M. Webb, MRC National Institute for Medical Research (London, UK), for providing the PBP clone and support in establishing the P_i release assay in our laboratory. We also thank R. Gasper for providing the Cdc42 protein and D. Vogt for technical support.

References

1. Bos, J. L., Rehmann, H. & Wittinghofer, A. (2007). GEFs and GAPs: critical elements in the control of small G proteins. *Cell*, **129**, 865–877.

† http://pymol.sourceforge.net

2. Vetter, I. R. & Wittinghofer, A. (2001). The guanine nucleotide-binding switch in three dimensions. *Science*, **294**, 1299–1304.
3. Gasper, R., Meyer, S., Gotthardt, K., Sirajuddin, M. & Wittinghofer, A. (2009). It takes two to tango: regulation of G proteins by dimerization. *Nat. Rev., Mol. Cell Biol.* **10**, 423–429.
4. Scheffzek, K., Ahmadian, M. R., Kabsch, W., Wiesmuller, L., Lautwein, A., Schmitz, F. & Wittinghofer, A. (1997). The Ras–RasGAP complex: structural basis for GTPase activation and its loss in oncogenic Ras mutants. *Science*, **277**, 333–338.
5. Rittinger, K., Walker, P. A., Eccleston, J. F., Smerdon, S. J. & Gamblin, S. J. (1997). Structure at 1.65 Å of RhoA and its GTPase-activating protein in complex with a transition-state analogue. *Nature*, **389**, 758–762.
6. Pan, X., Eathiraj, S., Munson, M. & Lambright, D. G. (2006). TBC-domain GAPs for Rab GTPases accelerate GTP hydrolysis by a dual-finger mechanism. *Nature*, **442**, 303–306.
7. Ismail, S. A., Vetter, I. R., Sot, B. & Wittinghofer, A. (2010). The structure of an Arf–ArfGAP complex reveals a Ca^{2+} regulatory mechanism. *Cell*, **141**, 812–821.
8. Veltel, S., Gasper, R., Eisenacher, E. & Wittinghofer, A. (2008). The retinitis pigmentosa 2 gene product is a GTPase-activating protein for Arf-like 3. *Nat. Struct. Mol. Biol.* **15**, 373–380.
9. Scrima, A., Thomas, C., Deaconescu, D. & Wittinghofer, A. (2008). The Rap–RapGAP complex: GTP hydrolysis without catalytic glutamine and arginine residues. *EMBO J.* **27**, 1145–1153.
10. Daumke, O., Weyand, M., Chakrabarti, P. P., Vetter, I. R. & Wittinghofer, A. (2004). The GTPase-activating protein Rap1GAP uses a catalytic asparagine. *Nature*, **429**, 197–201.
11. Burbelo, P. D., Drechsel, D. & Hall, A. (1995). A conserved binding motif defines numerous candidate target proteins for both Cdc42 and Rac GTPases. *J. Biol. Chem.* **270**, 29071–29074.
12. Bishop, A. L. & Hall, A. (2000). Rho GTPases and their effector proteins. *Biochem. J.* **348**, 241–255.
13. Rudolph, M. G., Bayer, P., Abo, A., Kuhlmann, J., Vetter, I. R. & Wittinghofer, A. (1998). The Cdc42/Rac interactive binding region motif of the Wiskott Aldrich syndrome protein (WASP) is necessary but not sufficient for tight binding to Cdc42 and structure formation. *J. Biol. Chem.* **273**, 18067–18076.
14. Thompson, G., Owen, D., Chalk, P. A. & Lowe, P. N. (1998). Delineation of the Cdc42/Rac-binding domain of p21-activated kinase. *Biochemistry*, **37**, 7885–7891.
15. Morreale, A., Venkatesan, M., Mott, H. R., Owen, D., Nietlispach, D., Lowe, P. N. & Laue, E. D. (2000). Structure of Cdc42 bound to the GTPase binding domain of PAK. *Nat. Struct. Biol.* **7**, 384–388.
16. Kim, A. S., Kakalis, L. T., Abdul-Manan, N., Liu, G. A. & Rosen, M. K. (2000). Autoinhibition and activation mechanisms of the Wiskott–Aldrich syndrome protein. *Nature*, **404**, 151–158.
17. Mott, H. R., Owen, D., Nietlispach, D., Lowe, P. N., Manser, E., Lim, L. & Laue, E. D. (1999). Structure of the small G protein Cdc42 bound to the GTPase-binding domain of ACK. *Nature*, **399**, 384–388.
18. Zheng, Z. L. & Yang, Z. (2000). The Rop GTPase: an emerging signaling switch in plants. *Plant Mol. Biol.* **44**, 1–9.
19. Berken, A. (2006). ROPs in the spotlight of plant signal transduction. *Cell. Mol. Life Sci.* **63**, 2446–2459.
20. Berken, A. & Wittinghofer, A. (2008). Structure and function of Rho-type molecular switches in plants. *Plant Physiol. Biochem.* **46**, 380–393.
21. Lee, Y. J. & Yang, Z. (2008). Tip growth: signaling in the apical dome. *Curr. Opin. Plant Biol.* **11**, 662–671.
22. Mucha, E., Fricke, I., Schaefer, A., Wittinghofer, A. & Berken, A. (2011). Rho proteins of plants—functional cycle and regulation of cytoskeletal dynamics. *Eur. J. Cell Biol.* doi:10.1016/j.ejcb.2010.11.009.
23. Christensen, T. M., Vejlupkova, Z., Sharma, Y. K., Arthur, K. M., Spatafora, J. W., Albright, C. A. *et al.* (2003). Conserved subgroups and developmental regulation in the monocot *rop* gene family. *Plant Physiol.* **133**, 1791–1808.
24. Hwang, J. U., Vernoud, V., Szumlanski, A., Nielsen, E. & Yang, Z. (2008). A tip-localized RhoGAP controls cell polarity by globally inhibiting Rho GTPase at the cell apex. *Curr. Biol.* **18**, 1907–1916.
25. Schaefer, A., Hoehner, K., Berken, A. & Wittinghofer, A. (2011). The unique plant RhoGAPs are dimeric and contain a CRIB motif required for affinity and specificity towards cognate small G proteins. *Biopolymers*, **95**, 420–433.
26. Wu, G., Li, H. & Yang, Z. (2000). *Arabidopsis* RopGAPs are a novel family of rho GTPase-activating proteins that require the Cdc42/Rac-interactive binding motif for rop-specific GTPase stimulation. *Plant Physiol.* **124**, 1625–1636.
27. Klahre, U. & Kost, B. (2006). Tobacco RhoGTPase ACTIVATING PROTEIN1 spatially restricts signaling of RAC/Rop to the apex of pollen tubes. *Plant Cell*, **18**, 3033–3046.
28. Borg, S., Podenphant, L., Jensen, T. J. & Poulsen, C. (1999). Plant cell growth and differentiation may involve GAP regulation of Rac activity. *FEBS Lett.* **453**, 341–345.
29. Abbal, P. & Tesniere, C. (2010). Putative *Vitis vinifera* Rop- and Rab-GAP-, GEF-, and GDI-interacting proteins uncovered with novel methods for public genomic and EST database analysis. *J. Exp. Bot.* **61**, 65–74.
30. Baxter-Burrell, A., Yang, Z., Springer, P. S. & Bailey-Serres, J. (2002). RopGAP4-dependent Rop GTPase rheostat control of *Arabidopsis* oxygen deprivation tolerance. *Science*, **296**, 2026–2028.
31. Fu, Y., Wu, G. & Yang, Z. (2001). Rop GTPase-dependent dynamics of tip-localized F-actin controls tip growth in pollen tubes. *J. Cell Biol.* **152**, 1019–1032.
32. Brune, M., Hunter, J. L., Corrie, J. E. & Webb, M. R. (1994). Direct, real-time measurement of rapid inorganic phosphate release using a novel fluorescent probe and its application to actomyosin subfragment 1 ATPase. *Biochemistry*, **33**, 8262–8271.
33. Brune, M., Hunter, J. L., Howell, S. A., Martin, S. R., Hazlett, T. L., Corrie, J. E. & Webb, M. R. (1998). Mechanism of inorganic phosphate interaction with phosphate binding protein from *Escherichia coli*. *Biochemistry*, **37**, 10370–10380.

34. Graham, D. L., Eccleston, J. F. & Lowe, P. N. (1999). The conserved arginine in rho-GTPase-activating protein is essential for efficient catalysis but not for complex formation with Rho·GDP and aluminum fluoride. *Biochemistry*, **38**, 985–991.
35. Mazhab-Jafari, M. T., Marshall, C. B., Smith, M., Gasmi-Seabrook, G. M., Stambolic, V., Rottapel, R. *et al.* (2010). Real-time NMR study of three small GTPases reveals that fluorescent 2′(3′)-*O*-(*N*-methylanthraniloyl)-tagged nucleotides alter hydrolysis and exchange kinetics. *J. Biol. Chem.* **285**, 5132–5136.
36. Ahmadian, M. R., Stege, P., Scheffzek, K. & Wittinghofer, A. (1997). Confirmation of the arginine-finger hypothesis for the GAP-stimulated GTP-hydrolysis reaction of Ras. *Nat. Struct. Biol.* **4**, 686–689.
37. Eberth, A., Dvorsky, R., Becker, C. F., Beste, A., Goody, R. S. & Ahmadian, M. R. (2005). Monitoring the real-time kinetics of the hydrolysis reaction of guanine nucleotide-binding proteins. *Biol. Chem.* **386**, 1105–1114.
38. Hemsath, L., Dvorsky, R., Fiegen, D., Carlier, M. F. & Ahmadian, M. R. (2005). An electrostatic steering mechanism of Cdc42 recognition by Wiskott–Aldrich syndrome proteins. *Mol. Cell*, **20**, 313–324.
39. Kraemer, A., Brinkmann, T., Plettner, I., Goody, R. & Wittinghofer, A. (2002). Fluorescently labelled guanine nucleotide binding proteins to analyse elementary steps of GAP-catalysed reactions. *J. Mol. Biol.* **324**, 763–774.
40. Kötting, C., Blessenohl, M., Suveyzdis, Y., Goody, R. S., Wittinghofer, A. & Gerwert, K. (2006). A phosphoryl transfer intermediate in the GTPase reaction of Ras in complex with its GTPase-activating protein. *Proc. Natl Acad. Sci. USA*, **103**, 13911–13916.
41. Chakrabarti, P. P., Daumke, O., Suveyzdis, Y., Kötting, C., Gerwert, K. & Wittinghofer, A. (2007). Insight into catalysis of a unique GTPase reaction by a combined biochemical and FTIR approach. *J. Mol. Biol.* **367**, 983–995.
42. Phillips, R. A., Hunter, J. L., Eccleston, J. F. & Webb, M. R. (2003). The mechanism of Ras GTPase activation by neurofibromin. *Biochemistry*, **42**, 3956–3965.
43. Lamson, R. E., Winters, M. J. & Pryciak, P. M. (2002). Cdc42 regulation of kinase activity and signaling by the yeast p21-activated kinase Ste20. *Mol. Cell. Biol.* **22**, 2939–2951.
44. Abdul-Manan, N., Aghazadeh, B., Liu, G. A., Majumdar, A., Ouerfelli, O., Siminovitch, K. A. & Rosen, M. K. (1999). Structure of Cdc42 in complex with the GTPase-binding domain of the 'Wiskott–Aldrich syndrome' protein. *Nature*, **399**, 379–383.
45. Scheffzek, K. & Ahmadian, M. R. (2005). GTPase activating proteins: structural and functional insights 18 years after discovery. *Cell. Mol. Life Sci.* **62**, 3014–3038.
46. Kötting, C., Kallenbach, A., Suveyzdis, Y., Wittinghofer, A. & Gerwert, K. (2008). The GAP arginine finger movement into the catalytic site of Ras increases the activation entropy. *Proc. Natl Acad. Sci. USA*, **105**, 6260–6265.
47. Rittinger, K., Walker, P. A., Eccleston, J. F., Nurmahomed, K., Owen, D., Laue, E. *et al.* (1997). Crystal structure of a small G protein in complex with the GTPase-activating protein rhoGAP. *Nature*, **388**, 693–697.
48. Zutz, A., Gompf, S., Schagger, H. & Tampe, R. (2009). Mitochondrial ABC proteins in health and disease. *Biochim. Biophys. Acta*, **1787**, 681–690.
49. Procko, E., Ferrin-O'Connell, I., Ng, S. L. & Gaudet, R. (2006). Distinct structural and functional properties of the ATPase sites in an asymmetric ABC transporter. *Mol. Cell*, **24**, 51–62.
50. Zaitseva, J., Oswald, C., Jumpertz, T., Jenewein, S., Wiedenmann, A., Holland, I. B. & Schmitt, L. (2006). A structural analysis of asymmetry required for catalytic activity of an ABC-ATPase domain dimer. *EMBO J.* **25**, 3432–3443.